Phosphatidylinositol-Specific Phospholipase C: Kinetic and Stereochemical Evidence for an Interaction between Arginine-69 and the Phosphate Group of Phosphatidylinositol[†,‡]

Robert J. Hondal,[§,||] Suzette R. Riddle,[§,||] Alexander V. Kravchuk,[§] Zhong Zhao,[§] Hua Liao,[§] Karol S. Bruzik,[⊥] and Ming-Daw Tsai*[,§]

Departments of Chemistry and Biochemistry and Ohio State Biochemistry Program, The Ohio State University, Columbus, Ohio 43210, and Department of Medicinal Chemistry and Pharmacognosy, College of Pharmacy, University of Illinois at Chicago, Chicago, Illinois 60612

Received November 19, 1996; Revised Manuscript Received January 29, 1997[⊗]

ABSTRACT: A new substrate analogue, (2*R*)-1,2-dipalmitoyloxypropanethiophospho-1-D-*myo*-inositol (DPsPI), has been used in a new, continuous assay for phosphatidylinositol-specific phospholipase C (PI-PLC). DPsPI is superior to other substrate analogs that have been used for assaying PI-PLC since it is synthesized as a pure diastereomer and maintains both acyl chains of the natural substrate, dipalmitoylphosphatidylinositol (DPPI). The assay that has been developed using this new analogue has allowed us to elucidate detailed kinetic data so far lacking in the field. In addition, several mutants of PI-PLC were constructed and assayed. The results show that Arg-69 is essential for catalysis, since mutations at this position led to a 10^3-10^4-fold decrease in activity with respect that of to the wild-type (WT) enzyme. An alanine mutant of Asp-67, a residue also found at the active site, displays activity similar to that of WT. We have also used nuclear magnetic resonance (NMR) and circular dichroism (CD) spectroscopy to analyze the structural integrity and conformational stability of the mutants. The results show that the overall global conformation of the enzyme is not perturbed by the mutants. The $^{15}N-^{1}H$ HSQC NMR spectrum of WT PI-PLC is also reported at 600 MHz. The stereoselectivity of the reaction toward the stereoisomers of another analogue, 1,2-dipalmitoyl-*sn*-glycero-3-thiophospho-1-*myo*-inositol (DPPsI), was used to probe whether Arg-69 interacts with the phosphate moiety of the substrate. We have calculated that the WT enzyme shows a stereoselectivity ratio of 160000:1 in favor of the R_p isomer versus the S_p isomer. The R69K mutant displayed a significant 10^4-fold relaxation of stereoselectivity. Our data support the role of Arg-69 in stabilizing the negative charge on the pentacoordinate phosphate in the transition state during catalysis.

Although inositol phospholipids constitute 10% or less of the total phospholipids in membranes of mammalian cells, phosphatidylinositols are a physiologically important class of biomolecules because of their significant role in signal transduction and cell signaling pathways (Rana & Hokin, 1990; Dennis et al., 1991). In addition, glycosylated PI[1] can serve as a membrane anchor for many proteins (Low, 1990).

So far, two families of phosphatidylinositol-specific phospholipase C (PI-PLC) enzymes have been identified, the eukaryotic or mammalian family and the bacterial family (Ikezawa, 1991; Lee et al., 1995; Rhee et al., 1989). PI-PLCs from both sources are extremely specific for *myo*-inositol phospholipids. Eukaryotic enzymes, however, will accept a multiply phosphorylated inositol ring, whereas the bacterial enzymes will not (Bruzik & Tsai, 1994). Bacterial PI-PLCs will also cleave the glycosyl-PI-containing membrane anchors of membrane proteins (Low & Saltiel, 1988). The reactions catalyzed by enzymes from both families are thought to share a common catalytic mechanism since they proceed through a common steric course at the phosphorus center (Bruzik et al., 1992) and also display a region of amino acid homology, the X domain, found in both classes of enzymes (Rhee et al., 1989). The *Bacillus thuringiensis* PI-PLC hydrolyzes PI to IP in two distinct steps (Figure 1). The conversion of PI to IcP is about 1000-fold faster than

† This work was supported by a grant from the National Institutes of Health (GM30327). The DMX-600 NMR spectrometer used was funded in part by NIH Grant RR08299 and NSF Grant BIR-9221639.

‡ This paper is dedicated to our colleague and friend, Conor R. O'Hanlon, who was working on the synthesis of our substrate analog before his death earlier this year.

* Address correspondence to this author at the Department of Chemistry.

§ The Ohio State University.

|| The first two authors of this paper contributed equally.

⊥ University of Illinois at Chicago.

⊗ Abstract published in *Advance ACS Abstracts,* March 1, 1997.

[1] Abbreviations: AMPS, adenosine 5′-monothiophosphate; ADPαS, adenosine 5′-*O*-(1-thiodiphosphate); CD, circular dichroism; CAPS, 3-(cyclohexylamino)propanesulfonic acid; *cis*-IcPs, *cis*-inositol 1,2-cyclic phosphorothioate; DHPC, diheptanoyl-*sn*-glycero-3-phosphocholine; DPPI, dipalmitoylphosphatidylinositol; DPPsI, 1,2-dipalmitoyl-*sn*-glycero-3-thiophospho-1-*myo*-inositol; DPsPI, (2*R*)-1,2-dipalmitoyloxypropanethiophospho-1-D-*myo*-inositol; DTNB, 5,5′-dithiobis(2-nitrobenzoic acid); DTP, 4,4′-dithiobispyridine; EDTA, ethylenediaminetetraacetic acid; Gdn-HCl, guanidinium chloride; HSQC, heteronuclear single-quantum coherence; C_{16}S-PI, hexadecylthiophosphoryl-1-*myo*-inositol; HEPES, *N*-(2-hydroxyethyl)piperazine-*N*′-2-ethanesulfonic acid; IcP, inositol 1,2-cyclic phosphate; IP, inositol 1-phosphate; $K_{m,app}$, apparent K_m; k_{R_p}, second-order rate constant for the R_p isomer of DPPsI; k_{S_p}, second-order rate constant for the S_p stereoisomer of DPPsI; substrate K_s, substrate dissociation constant from enzyme; MES, 2-(*N*-morpholino)ethanesulfonic acid; MOPS, 3-(*N*-morpholino)propanesulfonic acid; NPIP, *myo*-inositol 1-(4-nitrophenyl phosphate); [^{3}H]PI, L-α-[*myo-inositol*-2-^{3}H]phosphatidylinositol; NOESY, nuclear Overhauser enhancement spectroscopy; PI, phosphatidylinositol; PI-PLC, phosphatidylinositol-specific phospholipase C; PAGE, polyacrylamide gel electrophoresis; SDS, sodium dodecyl sulfate; STII, *Escherichia coli* heat stable enterotoxin signal sequence; *trans*-IcPs, *trans*-inositol 1,2-cyclic phosphorothioate; Tris, 2-amino-2-(hydroxymethyl)-1,3-propanediol; u, units; WT, wild-type.

S0006-2960(96)02866-8 CCC: $14.00

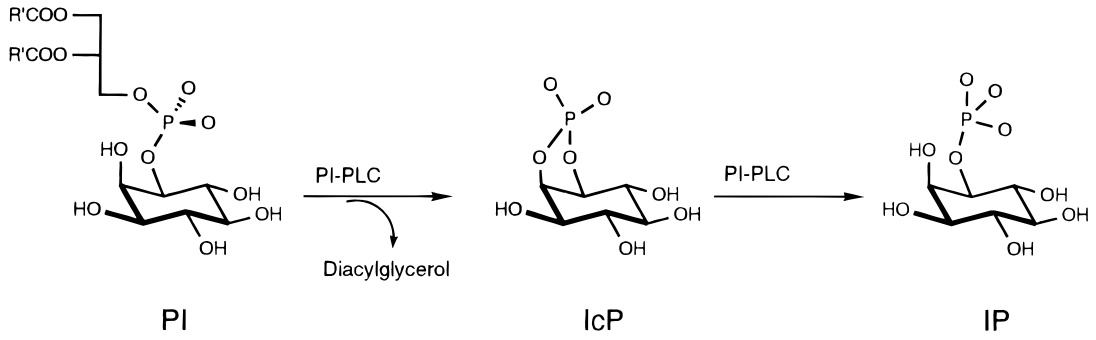

FIGURE 1: Conversion of phosphatidylinositol to IcP and IP catalyzed by PI-PLC.

the conversion of IcP to IP (Volwerk et al., 1990). The same catalytic residues are believed to be involved in both steps (Heinz et al., 1995). Eukaryotic PI-PLCs, however, release both IcP and IP simultaneously (Lee et al., 1995).

Recently, the crystal structure of PI-PLC from *Bacillus cereus* was published (Heinz et al., 1995). The structure supports the hypothesis (Bruzik et al., 1991) that the reaction proceeds through a mechanism similar to that of ribonuclease A (Richards & Wyckoff, 1971) in which two histidines act as a general acid and general base pair that switch roles in the first and second halves of the reaction. Mutagenesis studies have confirmed the importance of these two histidines in both mammalian and bacterial PI-PLCs (Cheng et al., 1995; Ellis et al., 1995; Heinz et al., 1995). The structure of mammalian PI-PLCδ (Essen et al., 1996) shows that the catalytic domain of the enzyme shares the $\alpha-\beta$ barrel structure of the bacterial enzyme.

We have chosen to study a bacterial enzyme rather than a eukaryotic enzyme because the bacterial enzyme is smaller, 35 kDa (Ikwasaki et al., 1994; Daugherty & Low, 1992; Kuppe et al., 1989), compared to 85−160 kDa for eukaryotic enzymes (Rhee & Choi, 1992). It allows quantitative analysis of the catalytic mechanism without being complicated by the regulatory regions which the mammalian enzymes have. Though the physiological functions of bacterial PI-PLCs are not fully understood, we believe that the mechanistic, stereochemical, and kinetic data from the bacterial enzymes can serve as a paradigm for their eukaryotic cousins.

As has been previously noted (Bruzik & Tsai, 1994), a standard and accurate assay method for PI-PLCs is needed to elucidate detailed kinetic and mechanistic information. We herein present the development of a new continuous spectrophotometric assay for PI-PLC based on the thiophosphate PI analogue, (2*R*)-1,2-dipalmitoyloxypropanethiophospho-1-D-*myo*-inositol (DPsPI). DPsPI is an excellent analogue that allows the reaction to be assayed in a continuous manner, a marked improvement over previously used specific activity assays.

NMR, CD, and the above-mentioned assay were used to study the properties of wild-type PI-PLC. In addition, site-directed mutagenesis was used to probe the structural and functional roles of Asp-67 and Arg-69. The crystal structure of the PI-PLC·*myo*-inositol complex shows that these residues are located at the active site of the enzyme (Figure 2), and it had been suggested by the authors that the role of Arg-69 during catalysis was to stabilize the negative charge on the pentacoordinate phosphate in the transition state (Heinz et al., 1995). The kinetic data demonstrate that Arg-69 is essential for catalysis, while the structural data obtained by CD and NMR spectroscopy indicate that the overall conformation of the mutants is not changed with respect to WT. We have also used the stereoisomers of another substrate analogue, 1,2-dipalmitoyl-*sn*-glycero-3-thiophospho-1-*myo*-inositol (DPPsI), to probe the role of Arg-69 in catalysis. The results of the stereochemical data indicate that PI-PLC is highly specific for the R_p isomer of DPPsI and Arg-69 plays an important role in determining which stereoisomer is converted to the product.

MATERIALS AND METHODS

Materials. Phosphatidylinositol from bovine brain was purchased from Avanti Polar Lipids. L-α-[*myo*-inositol-2-^{3}H]Phosphatidylinositol was purchased from Dupont NEN. DEAE-cellulose was purchased from Whatman. Sodium deoxycholate, Sephadex G-100, and crude L-α-PI were purchased from Sigma. Phenyl-Sepharose and AG-8X (formate form) resin were purchased from BioRad. All restriction and DNA modification enzymes were purchased from either New England BioLabs, Boehringer Mannheim, or United States Biochemicals. Vent polymerase was purchased from New England Biolabs. pET-21-b was purchased from Novagen. pHN1403 was a generous gift from F. Dahlquist. pMY31 was a generous gift from J. Volwerk. Sequencing and mutagenesis kits were purchased from United States Biochemicals, Amersham, and Applied Biosystems. Mutagenic primers were purchased from The Midland Certified Reagent Co. and Integrated DNA Technologies, Inc. ^{15}N-labeled ammonium sulfate was purchased from Isotech, Inc. Formula 989 scintillation cocktail was purchased from Dupont NEN. Cuvettes were purchased from Starna Cells, Inc. All chemicals were purchased from Sigma Chemical, Aldrich, Fisher, or Research Organics unless otherwise specified.

Construction of Expression Vectors and Purification of PI-PLC. To improve the expression of *B. thuringiensis* PI-PLC in *Escherichia coli*, we cloned the PI-PLC gene, with the STII signal sequence into the plasmid pHN1403, which uses a *lac-tac-tac* promoter, using the *Xba*I and *Sph*I sites found on both vectors. To express PI-PLC, we transformed the *E. coli* cell strain MM294 with pHN1403-PIPLC using the standard $CaCl_2$ method (Sambrook et al., 1989). For mutagenesis, the PI-PLC gene was subcloned into M13mp19. Mutagenesis was performed using site-specific primers and the *Sculptor* mutagenesis kit from Amersham.

An additional expression vector, pET-21-b-PLC, was constructed for expression of PI-PLC in minimal media since the *E. coli* strain MM294 did not grow in minimal media

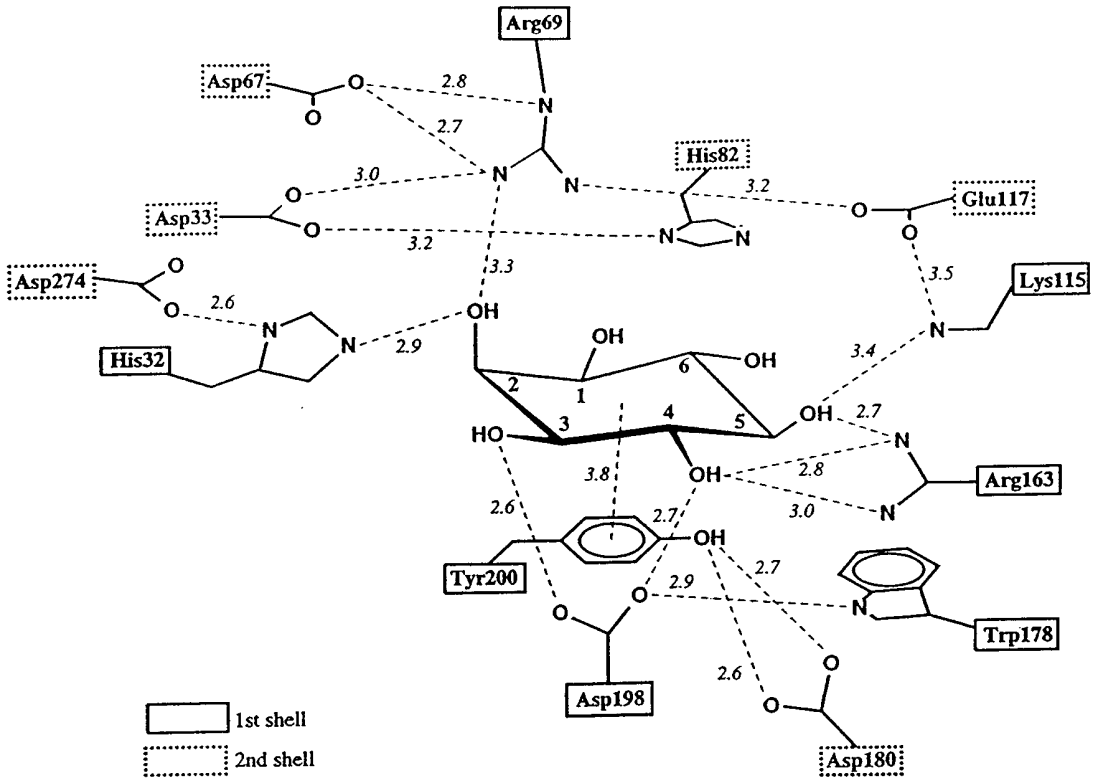

FIGURE 2: Active site structure of *B. cereus* PI-PLC. Reproduction of Figure 7 from Heinz et al. (1995). Copyright 1995 Oxford University Press.

and, when other strains of *E. coli* were used, the expression of PI-PLC was much lower or nonexistent. The pET-21-b-PLC plasmid was constructed by cloning the *B. thuringiensis* PI-PLC gene and the STII signal sequence into pET-21-b using *Nde*I and *Sal*I restriction sites. These restriction sites were engineered at a location adjacent to the coding region by incorporating them into the oligonucleotides used to amplify the coding region via the polymerase chain reaction. Both the upstream primer, 5′-AACAGACATATGAAAAAGAATATCGCATTTCTTC-3′ (*Nde*I site underlined), and the downstream primer, 5′-AACAGACATATGAAAAAGAATATCGCATTTCTTC-3′ (*Sal*I site underlined), contain additional nucleotides at their 5′ ends that act as clamping sequences to aid in optimal digestion. The PI-PLC coding region was amplified using 50 pmol each of upstream and downstream primer, 150 ng of M13-PLC (replicative form) DNA as the template, each dNTP (200 μM), 2 units of Vent polymerase, 10 mM KCl, 10 mM $(NH_4)_2SO_4$, 20 mM Tris-HCl (pH 8.8), 2 mM $MgSO_4$, and 0.01% Triton X-100 in a final reaction volume of 100 μL. Thermal cycle parameters were 96 °C for 2 min (initial denaturation), followed by 18 cycles of 45 s at 96 °C (denaturation), 30 s at 55 °C (annealing), and 1 min at 73 °C (extension). Cycling was performed on a Perkin-Elmer 480 thermal cycler. The PCR product was then purified using a Microcon 100 apparatus (Amicon), digested by restriction enzymes, and ligated to pET-21-b cut with the same restriction enzymes. Positive clones were screened by restriction digestion and sequenced to verify the entire sequence.

The expression of PI-PLC was carried out by inoculating 10 L of LB with stationary phase MM294/pHN1403-PIPLC and growing to an OD of 1.0 at 34 °C, before inducing with 1 mM IPTG. After that, the cells were grown for another 12 h at 30 °C and then harvested by centrifugation at 2200*g* for 15 min. To remove excess media from the cells, they were washed in 20 mM Tris (pH 7.5) and 50 mM NaCl prior to being stored at −20 °C which weakened the cell membranes in preparation for extraction. PI-PLC was extracted from the harvested cells by sonication in 8.1 mL of 20 mM Tris-HCl buffer (pH 8.5) per gram of cell pellet. The extracted protein is separated from the cellular debris by centrifugation at 14000*g* for 25 min. The extract is loaded onto a 200 mL DEAE-cellulose column pre-equilibrated in 20 mM Tris-HCl (pH 8.5). After thorough washing with 50 mM NaCl (30 mM for D67A), the column is eluted with a 1200 mL gradient of 50 to 200 mM NaCl. Fifteen milliliter fractions are collected and analyzed for PI-PLC by absorbance at 280 nm and SDS−PAGE. The fractions containing PI-PLC are pooled and precipitated with ammonium sulfate at 90% saturation. The precipitated protein is resuspended in a minimum volume of 20 mM Tris (pH 8.5) and loaded onto a 500 mL pre-equilibrated Sephadex G-100 column. PI-PLC is eluted off in the same buffer and collected in 5 mL fractions, which are analyzed as above. The fractions containing PI-PLC are pooled, brought to a 1.2 M NaCl concentration, and loaded onto a 20 mL phenyl-Sepharose column, pre-equilibrated in 20 mM Tris (pH 8.5) and 1.2 M NaCl. After the column is washed with the equilibration buffer, PI-PLC is eluted off the column with a 1.2 to 0 M NaCl gradient followed by a no salt wash. PI-PLC elutes at the end of the gradient and into the beginning of the wash. Again, the fractions containing PI-PLC are pooled and concentrated to a final volume of 5−10 mL. PI-PLC is then dialyzed twice against 8 L of 0.1 mM HEPES buffer (pH 7) and lyophilized for storage at −20 °C. All handling of the enzyme was done at 4 °C, and all buffers were pH adjusted at 4 °C.

The expression of pET-21-b-PLC was carried out by inducing BL21(DE3) cells containing pET-21-b-PLC at an OD of 0.8 with 1 mM IPTG and then growing for another 4 h at 37 °C. Cells were grown in M9 minimal media with $(^{15}NH_4)_2SO_4$ (99.4 at. % ^{15}N) as the only nitrogen source. Purification for the ^{15}N-labeled protein was the same as for PI-PLC expressed in pHN1403-PIPLC.

Assays. Several assay methods were performed to determine the activities of both the WT and mutant PI-PLCs. The enzymes' specific activities toward PI were determined using a minor modification of the assay developed by Griffith et al. (1991). First, L-α-[*myo*-inositol-2-^{3}H]phosphatidylinositol ([^{3}H]PI) was mixed with unlabeled PI to give a specific activity of 1 250 000 cpm/μmol and an overall PI concentration of 10 mM, which is then sonicated using a Branson model 1210 water bath sonicator for 5−10 min to ensure micelle formation. The reaction mixture consisted of 20 μL of this suspension, 20 μL of 0.8% sodium deoxycholate, and 40 μL of 0.1 M sodium borate (pH 7.5). PI-PLC was diluted in 20 mM sodium borate (pH 7.5) to the appropriate concentration so that the reaction did not exceed 30% conversion of PI to IcP. Once diluted, 20 μL of PI-PLC was added to the reaction mixture and incubated at 37 °C for 10 min. The reaction was quenched with the addition of 500 μL of $CHCl_3$/MeOH/HCl (66:33:1). After brief centrifugation to separate the phases, 50 μL of the aqueous phase was counted for 10 min on a Beckman LSC3801 scintillation counter with a channel setting of 0−400. The activity was calculated in terms of units per milligram (1 U = 1 μmol min^{-1}). The concentration of PI-PLC was calculated using the extinction coefficient of 64 000 M^{-1} cm^{-1} reported by Volwerk et al. (1994).

Continuous Assay for PI Conversion to IcP. In addition to the specific activity for PI, mutant enzymes that did not have greatly (10^{-4} or less) decreased levels of activity were assayed using a new spectrophotometric assay. In this assay, a thiophosphate PI analogue, (2*R*)-1,2-dipalmitoyloxypropanethiophospho-1-D-*myo*-inositol (DPsPI), is used to measure the reaction rate. Synthesis of this substrate will be detailed elsewhere (K. S. Bruzik et al., unpublished results). This allows cleavage of the inositol moiety to be measured in a continuous manner by following the subsequent reaction of the free thiol with 5,5′-dithiobis(2-nitrobenzoic acid) (DTNB). The spectrophotometric method is a modification of the one reported by Hendrickson and Dennis (1984). A stock of concentrated DPsPI solution containing 2.20 mM DPsPI and 8.80 mM DHPC in buffer (50 mM MOPS at pH 7.5) was prepared for several sets of assays by the following procedure. A measured amount of DPsPI was dissolved in chloroform/methanol, and the solution was dried under a stream of argon and then *in vacuo* for 10 min. MOPS buffer and 50 mM DHPC in MOPS buffer were added to achieve the desired final concentrations; the mixture was vortexed briefly and then sonicated for 5 min at room temperature to completely solubilize the lipid. The stock solution was diluted with MOPS buffer (50 mM) into different concentrations (0−2.0 mM) prior to assaying. Diluted substrate solution (225 μL) was placed in a microcuvette (2 × 10 mm), and 5 μL of 50 mM DTNB in ethanol was added, stirred well with a gel-loading tip on a Pipetteman (Ranin Instruments, Inc.), avoiding bubbles. The microcuvette was equilibrated for 5 min at 25 °C in a UVIKON 930 spectrophotometer (Kontron Instruments). After equilibration, a background reaction rate was recorded for 2 min at 412 nm with a sampling rate of 150 with the spectrophotometer in the time drive mode. Five microliters of the appropriate concentration of PI-PLC (10 ng/μL WT) in 20 mM Tris and 2 mM EDTA (pH 7.5) was added and mixed quickly, and the absorbance was recorded for 2 min or more. The extinction coefficient (ϵ) of 12 800 M^{-1} cm^{-1} for 5-thio-2-nitrobenzoic acid (Yu & Dennis, 1991) was used to calculate enzyme activity. The initial reaction rate as a function of substrate concentration was treated by curve fitting of the data to the Michaelis−Menten equation using SigmaPlot (Jandel Corp.).

Structural Characterization. Both one-dimensional NMR and two-dimensional NOESY NMR spectra were taken of wild-type and mutant enzymes to determine the structural integrity of the mutants with respect to WT. NMR spectra were recorded on a Bruker DMX-600 NMR spectrometer at 310 K. PI-PLC was redissolved in 99.7% D_2O to a concentration of 0.2 mM and adjusted to pH 6.8 (direct pH meter reading). Chemical shifts were referenced to an internal sodium 3-(trimethylsilyl)propionate-2,2,3,3-d_4 standard. Two-dimensional NOESY spectra were acquired with a mixing time of 100 ms. The residual water signal was suppressed by a 3-9-19 pulse sequence with gradients (Piotto et al., 1992; Sklenar et al., 1993). A two-dimensional $^{15}N-^1H$ HSQC (Bodenhausen & Ruben, 1980; Bax et al., 1990) experiment was conducted using the sensitivity-enhanced method (Kay et al., 1992) on uniformly ^{15}N-labeled sample in 90% H_2O/10% D_2O.

In order to measure the conformational stability of the wild-type and mutant enzymes, a Gdn-HCl titration was performed using circular dichroism (CD) to follow the unfolding process. CD spectroscopy was performed on a JASCO-500C circular dichrometer. Spectra were recorded by scanning the spectrum between 220 and 210 nm, and the molar ellipticity was recorded at 215 nm. Protein solutions of 0.05 mg/mL were prepared in a buffer containing 10 mM sodium borate (pH 7.5) and 0.1 mM EDTA and then titrated with 0−4 M guanidinium chloride. $\Delta G_d^{H_2O}$ values were then calculated according to the method of Pace (1989).

Analysis of Stereochemistry by ^{31}P NMR. ^{31}P NMR spectra were taken on a Bruker AM-250 MHz spectrometer at a spectral frequency of 101.25 MHz. ^{31}P chemical shifts are referenced to external 85% H_3PO_4. DPPsI, 1,2-dipalmitoyl-*sn*-glycero-3-thiophospho-1-*myo*-inositol, was synthesized previously as described by Bruzik et al. (1991), as a mixture of the R_p and S_p stereoisomers. These stereoisomers of DPPsI were then used to probe the stereoselectivity of WT and mutant PI-PLCs. Assays were performed in a total volume of 0.5 mL containing 8.4 mM DPPsI (R_p plus S_p) and 40 mM sodium borate (pH 7.5) with varying amounts of WT and mutant PI-PLC. The DPPsI stereoisomers, R_p and S_p, were present in the reaction mixture as a 2:1 ratio of S_p to R_p isomers. DPPsI was prepared as mixed micelles with sodium deoxycholate. Sodium deoxycholate was chosen as the detergent since it is used in the specific activity assay. The ratio of sodium deoxycholate to DPPsI was 2:1.

RESULTS

Expression and Purification of WT PI-PLC. In order to purify sufficient protein for our kinetic and biophysical studies, we constructed an expression system improved

Table 1: Assay Results for Purified WT and PI-PLC Mutants

specific activity assay results		DPsPI assay results	
enyme	[^{3}H] PI (U/mg)	V_{max}[a]	K_m[b]
WT	1300	53.5	0.18
D67A	1890	107	0.23
R69A	0.024	ND	ND
R69K	1.0	0.03	0.8
R69M	0.013	ND	ND

[a] Units for V_{max} are micromoles per minute per milligram. [b] K_m is in millimolar. One U = 1 μmol/min. ND = not determined.

compared to that previously used with pMY31 (Koke et al., 1991). To do this, we cloned the *B. thuringiensis* PI-PLC gene and the STII signal sequence from pMY31 into the *lac-tac-tac* expression vector pHN1403 using the *Xba*I and *Sph*I sites found in both plasmids. Although expression levels of *B. thuringiensis* PI-PLC were only moderate, highly purified protein was obtained after three columns, a DEAE column, a Sephadex G-100 column, and a phenyl-Sepharose column. A silver nitrate-stained SDS−PAGE showed PI-PLC to be greater than 98% pure, and typical yields were 30−60 mg of protein from 10 L of cells. For storage, PI-PLC was extensively dialyzed against a weak buffer and lyophilized.

Unfortunately, we were unable to express PI-PLC from the pHN1403-PIPLC vector in minimal media as required for ^{15}N labeling experiments. In order to express PI-PLC in minimal media, we cloned the *B. thuringiensis* PI-PLC into pET-21-b. The ^{15}N-labeled PI-PLC was purified in the same manner as unlabeled PI-PLC.

Construction of D67 and R69 Mutants. The mutants D67A, R69A, R69M, and R69K were constructed using the *Sculptor* (Amersham) mutagenesis kit, mutant oligonucleotide primers, and the PI-PLC gene cloned into M13mp19. Mutations were confirmed by sequencing the gene after mutagenesis.

Specific Activities of WT and Mutants. The *B. thuringiensis* PI-PLC catalyzes the conversion of PI to IP in two different steps as shown in Figure 1. Several assay methods have been used so far to probe the activity of PI-PLCs. Since the conversion of PI to IcP is 1000-fold faster than the conversion of IcP to IP, most assays have focused on the conversion of PI to IcP. Most frequently used is a discontinuous assay in which the released cyclic intermediate is separated from the substrate in an aqueous phase and measured by either phosphate determination or more recently radioactivity (Griffith et al., 1991). We have used this method to assay both the wild-type and the mutant PI-PLCs. The results of this assay are presented in Table 1. The specific activity for our recombinant WT PI-PLC agrees well with previously reported values for the specific activity of bacterial PI-PLCs, 1200−1500 U/mg (Griffith et al., 1991).

Development of a Continuous Assay with DPsPI. In order to collect more detailed kinetic data on the hydrolysis of PI, it is desirable to use a continuous assay. We have developed a continuous spectrophotometric assay that uses (2*R*)-1,2-dipalmitoyloxypropanethiophospho-1-D-*myo*-inositol (DPsPI, Figure 3) as a substrate. The synthesis of DPsPI will be described elsewhere (Mihai et al., 1997). Upon reaction with PI-PLC, DPsPI is converted to cyclic inositol phosphate and thiodiacylglycerol. The thiol group on the thiodiacylglycerol then reacts with a coupling reagent, DTNB, allowing DPsPI

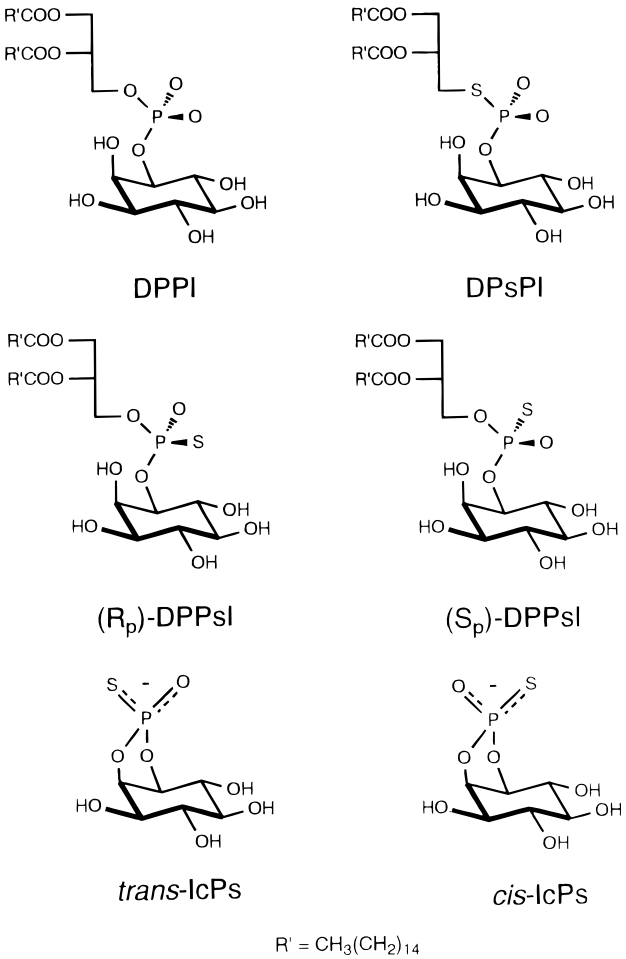

FIGURE 3: Structures of DPPI and the substrate analogues used in this study.

turnover to be calculated by measuring the increase of absorbance at 412 nm. The continuous assay of WT PI-PLC with DPsPI, in the form of mixed micelles with DHPC, was carried out with the concentration of DPsPI varied from 0 to 2 mM. The concentration of DHPC was 4 times that of DPsPI. DHPC was chosen as the detergent because it was found to be the best solubilizing agent for DPsPI. DHPC, because of its unique properties, has been found to be a superior detergent for many biological applications (Kessi et al., 1994). Without any detergent or DHPC present, the turnover of DPsPI by PI-PLC was undetectable. The assay time course was linear without a lag phase. Initial reaction rates were linear with respect to the amount of enzyme used in the assay (up to at least 100 ng of WT PI-PLC/assay) (Figure 4A). When 4,4′-dithiobispyridine (DTP) was used instead of DTNB as the coupling reagent, a similar rate was observed. Sodium deoxycholate and Triton X-100 were not as good as DHPC for solubilizing DPsPI, and the activities were considerably less than those with DHPC. A ratio of 1:4 DPsPI/DHPC for mixed micelles resulted in optimal PI-PLC activity. With this ratio of substrate to detergent, the plot of the initial reaction rate versus the bulk concentration of DPsPI resulted in a hyperbolic curve (Figure 4B). The enzyme became saturated at DPsPI concentrations above 2.0 mM. When DHPC was held at a constant concentration (8.1 mM) rather than at a constant ratio to DPsPI, a hyperbolic curve was also observed, but the saturating concentration appeared to be much higher as also

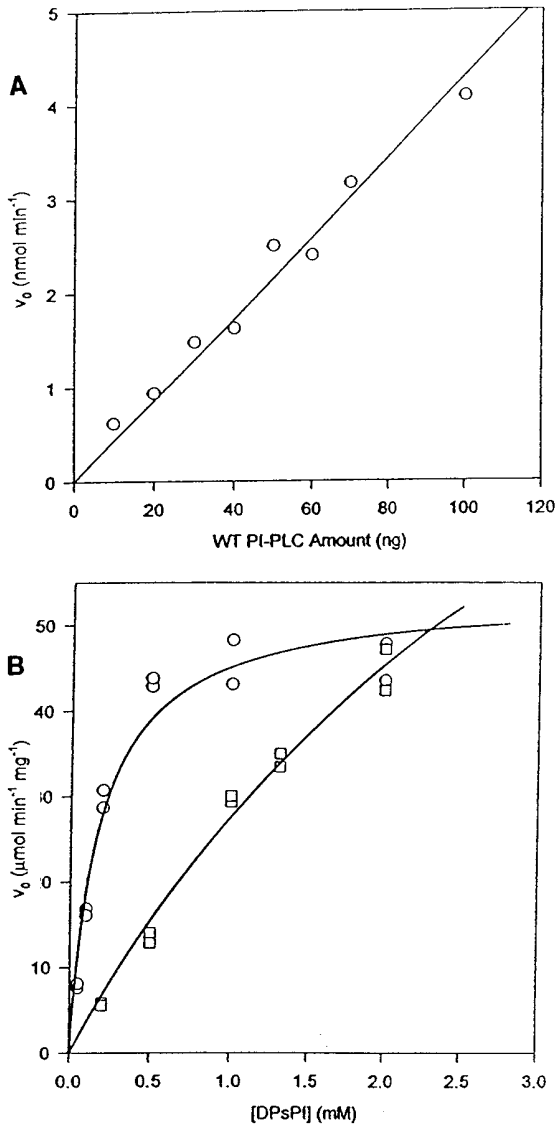

FIGURE 4: (A) Continuous assay of enzyme dependence. Initial reaction rate of WT PI-PLC as a function of the enzyme concentration used for each assay. The substrate is mixed micelles of DPsPI/DHPC at a ratio of 1:4. (B) Continuous assay of substrate dependence. Initial reaction rate of WT PI-PLC as a function of the concentration of DPsPI: (○) 1:4 DPsPI/DHPC and (□) 8.08 mM DHPC. The micelles were prepared in 50 mM MOPS at pH 7.5, and 1 mM DTNB was used as the coupling reagent.

shown in Figure 4B. Considering the amount of substrate needed to run each assay, we chose to hold the DPsPI:DHPC ratio constant at 1:4. Values of 53.5 μmol min^{-1} mg^{-1} for V_{max} and 0.18 mM for $K_{m,app}$ were obtained for WT PI-PLC under these conditions. All mutant assays were performed using the same conditions as those of WT. The kinetic data thus obtained are shown in Table 1.

Although the V_{max} values from the continuous assay are lower than the specific activities obtained by the radioactive assay, the two assays agree in the relative activities between WT and the mutants. R69K is 10^3-fold less active than WT, and D67A has an activity in the same range as that of WT. The alanine and methionine mutants of R69 have comparable levels of activity, approximately 50000-fold less than that of WT, and approximately 50-fold lower than that of R69K.

Structural Characterization by NMR. Since the essence of site-directed mutagenesis is the substitution of one amino acid with any other amino acid, it is important to confirm that the global structure of the protein is not changed. Two methods of structural characterization were employed. First, the one-dimensional NMR spectra (data not shown) and two-dimensional NOESY spectra (data not shown) of WT and mutant proteins were obtained. Little or no global conformational change of the mutant enzyme structures is indicated since the one-dimensional and two-dimensional NOESY NMR spectra of WT and the mutants are similar. To ensure that PI-PLC did not lose its structure during the 22 h NOESY experiment, a one-dimensional spectrum was taken of PI-PLC after the completion of the NOESY experiment; the spectrum was unchanged with respect to the spectrum taken prior to the NOESY experiment (data not shown). The only mutant with significant differences in its one-dimensional and two-dimensional NMR spectra is R69A, which has a slightly broader one-dimensional spectrum and fewer cross-peaks in its two-dimensional spectrum. The fact that observable NOE cross-peaks in the spectrum of the R69A mutant align quite well with the spectrum of WT suggests that differences in the spectra are due to higher flexibility and/or lower stability of the mutant and not to a global conformational change of the molecule.

In order to gain further structural information, and in pursuit of structure and dynamics of PI-PLC in solution, we obtained two-dimensional ^{15}N$-^{1}$H HSQC spectrum of uniformly ^{15}N-labeled enzyme (data not shown). Remarkably, for a protein of this size, signals from about 80% of backbone NH groups are observed even without deuteration. In agreement with a high content of β-sheets in the structure (Heinz et al., 1995), there is a large chemical shift dispersion of NH signals: 5.1−11.0 and 103−133 ppm in the ^{1}H and ^{15}N dimensions, respectively. Further work in this area is underway. None of the mutants presented in this study have significant perturbations in their one-dimensional and two-dimensional NMR spectra that would require further characterization by HSQC at this time.

Analysis of Conformational Stability by CD. We have used circular dichroism spectroscopy as a qualitative measure of secondary structures in comparing the mutants to WT. CD spectra of WT between 190 and 250 nm show two local minima, one near 214 nm and the other at 205 nm (data not shown). Similarly, the mutants show a very similar CD spectrum, with only R69A displaying a slightly more shallow spectrum. The conformational stabilities of the mutants and WT enzyme were determined by Gdn-HCl-induced denaturation measured CD spectroscopy. The denaturation curves of mutants and WT enzyme are shown in Figure 6 and display a behavior consistent with an apparent two-state folding mechanism. The denaturation data were fit with the following equation (Pace, 1989):

$$\Delta G_d = \Delta G_d^{H_2O} - m[\text{Gdn-HCl}]$$

where ΔG_d is the Gibbs free energy change at various concentrations of Gdn-HCl, $\Delta G_d^{H_2O}$ is the Gibbs free energy change at a zero concentration of Gdn-HCl, and m is a constant related to the susceptibility of the energy toward denaturation by the denaturant. A plot of ΔG_d versus Gdn-HCl concentration was then constructed. The $\Delta G_d^{H_2O}$ values

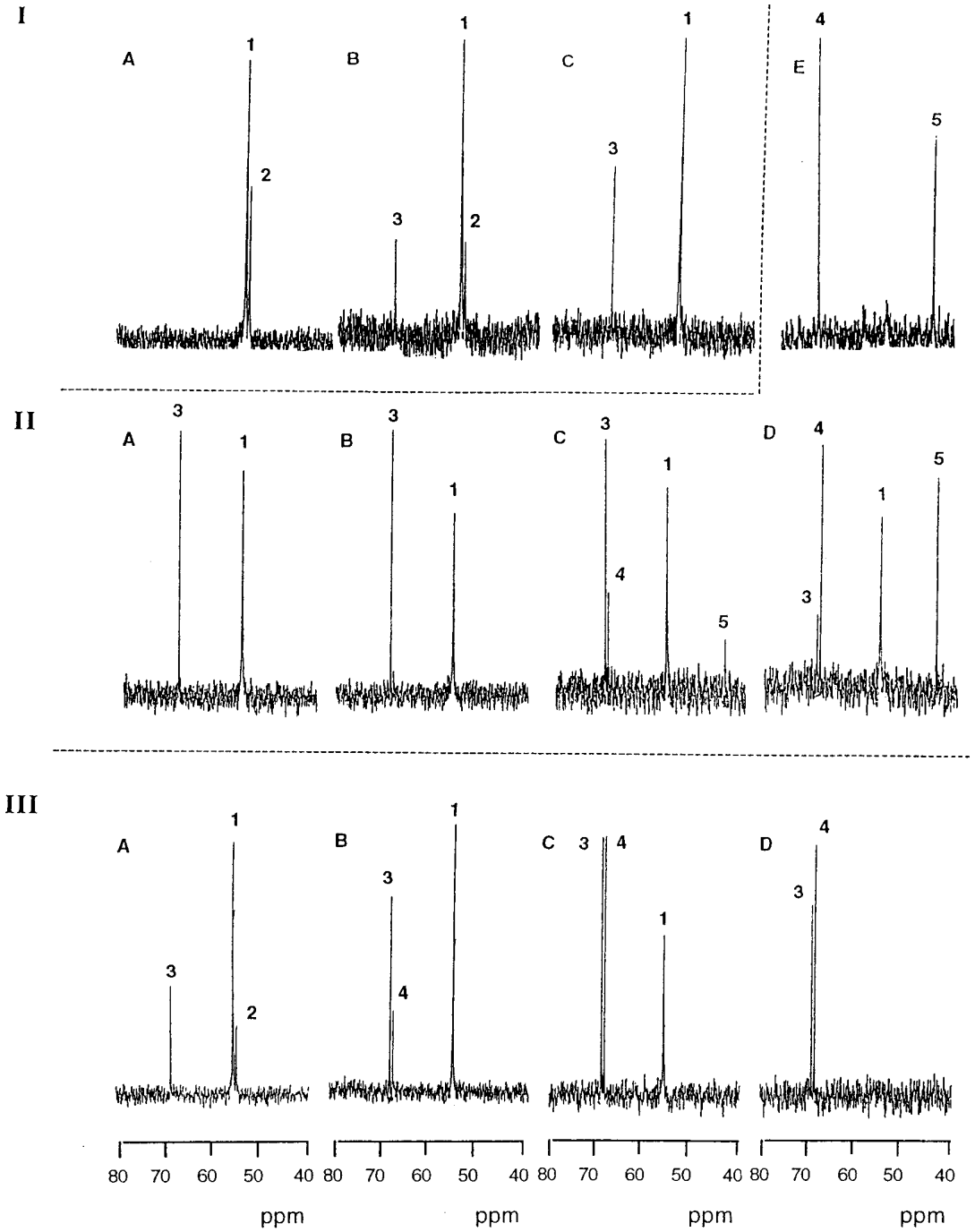

FIGURE 5: ^{31}P NMR analysis of the stereoselectivity of PI-PLC toward (R_p)- and (S_p)-DPPsI. (IA) ^{31}P NMR spectrum of the reaction mixture before addition of enzyme, showing a 2:1 mixture of the S_p isomer (peak 1) and the R_p isomer (peak 2). (IB) With 0.055 unit of WT enzyme added to IA, the spectrum is after 15 min (midpoint of the spectrum) of incubation with enzyme. Peak 3 is the *trans*-IcPs product which has been converted from the R_p isomer (peak 2). (IC) Spectrum taken after 84 min (midpoint) of incubation with 0.055 unit of WT. (IIA) At 15 min (midpoint) after addition of excess WT enzyme (195 units) added to the reaction mixture. (IIB) At 133 min (midpoint) after addition of excess WT addded to the reaction mixture. (IIC) At 450 min (midpoint) after addition of excess WT enzyme. Peak 4 is the *cis*-IcPs product which has been converted from the S_p isomer (peak 1). Peak 5 is 1-inositol phosphorothioate which has been converted from *trans*-IcPS (peak 3). (IID) At 72 h postincubation with excess WT enzyme. (IIE) The WT reaction from IID treated with an additional 275 units of WT. Peak 3 is *trans*-IcPs. Peak 4 is *cis*-IcPs. Peak 5 is 1-inositol phosphorothioate. (IIIA) Spectrum taken after 15 min (midpoint) with 0.45 unit of R69K added to the reaction mixture (spectrum IA). (IIIB) Spectrum taken after 133 min (midpoint) (R69K mutant). (IIIC) Spectrum taken 450 min (midpoint) postincubation with the R69K mutant (IIID) Spectrum taken after 48 h (R69K mutant).

and the slope (m) were determined from this plot. Those values, along with the midpoint of the denaturation curve ($D_{1/2}$), are listed in Table 2. The data suggest that the mutations at position 69 did not significantly alter the conformational stability. The D67A mutant shows the greatest perturbation in stability with respect to WT, though it is difficult to compare their $\Delta G_d^{H_2O}$ values because they have different values of m. The loss of the aspartate side chain, which is proposed to form a hydrogen bond with Arg-69, may cause the enzyme to be more susceptible to denaturation by Gdn-HCl, though its structure is not significantly disturbed as measured by CD and NMR spectroscopy.

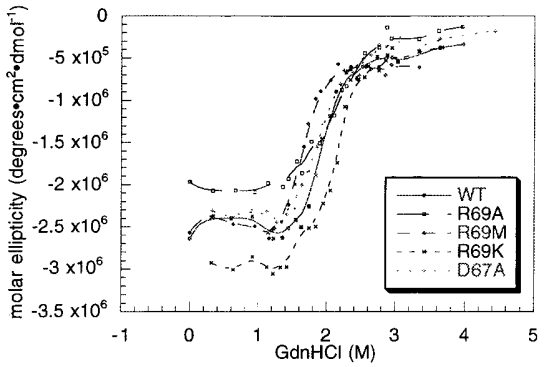

FIGURE 6: Denaturation curves for WT and mutants at various Gdn-HCl concentrations. Enzyme solutions containing 10 mM borate and 0.1 mM EDTA at pH 7.5 were incubated at 19 °C for 10 min and then scanned 10 times from 220 to 210 nm. The ellipticity at 215 nm was recorded.

Table 2: Free Energy of Gdn-HCl-Induced Denaturation for WT PI-PLC and Mutants[a]

enzyme	ΔG (kcal/mol)	m (kcal mol^{-1} M^{-1})	$D_{1/2}$ (M)
WT	7.0	−3.6	2.0
D67A	4.7	−2.4	1.9
R69A	5.9	−2.8	2.1
R69K	6.4	−2.8	2.3
R69M	6.5	−3.8	1.7

[a] The error limit in $\Delta G_d^{H_2O}$ is estimated to be ±0.5 kcal/mol.

Stereochemistry of WT and Mutant PI-PLC via ^{31}P NMR. The lack of structural perturbation in the mutants presented above and the decrease in the V_{max} of Arg-69 mutants allowed us to conclude that the side chain of Arg-69 is important for the catalysis by PI-PLC. However it does not address "how" it is involved in catalysis. To address this question, we examined the stereoselectivity of PI-PLC toward R_p and S_p isomers of DPPsI. It has been shown previously (Lin & Tsai, 1989) that PI-PLC is specific toward the R_p isomer of DPPsI. If the stereoselectivity is reversed or significantly relaxed in the mutant, it can be concluded that the arginine side chain interacts with the phosphate moiety of PI. Such an approach has been used previously to address enzyme−substrate interactions in adenylate kinase (Jiang et al., 1991; Dahnke et al., 1991).

Figure 5 (IA) shows the ^{31}P NMR spectrum of a mixture of the S_p and R_p isomers of DPPsI. The S_p isomer shows a signal at 55.9 ppm (peak 1), and the R_p isomer displays a signal slightly upfield at 55.2 ppm (peak 2), which agrees with previously assigned values (Lin & Tsai, 1989). Integration of the peaks reveals that the ratio of S_p to R_p is 2:1. Three sets experiments, **I**−**III**, were performed using the same amount of (R_pS_p)-DPPsI/sodium deoxycholate micelles. In the first experiment, a limiting amount of WT PI-PLC (0.055 unit) was added to the mixture of stereoisomers shown in Figure 5 (IA) and the time course of the reaction was then monitored by ^{31}P NMR. Time points in this experiment are shown in parts IB and IC of Figures 5. The R_p isomer is selectively converted to peak 3 at 69.9 ppm, which has been assigned as *trans*-inositol 1,2-cyclic phosphorothioate (*trans*-IcPs) (Lin & Tsai, 1989) (see Figure 3 for the structure). In the second experiment (IIA−IIE), an excess amount of WT enzyme (195 units) was used in an attempt to convert the S_p isomer to the *cis*-inositol 1,2-cyclic phosphorothioate (*cis*-IcPs) product. A peak corresponding to the *cis*-IcPs product (peak 4) is clearly visible in Figure 5 (IIC). Further incubation led to the conversion of peak 3 to 1-inositol phosphorothioate (IPs) (peak 5), as shown in Figure 5 (IID). Much of the S_p isomer is still remaining even after 72 h [Figure 5 (IID)]. It takes an additional 275 units of WT PI-PLC to finish the conversion of the S_p isomer into product [Figure 5 (IIE)]. The *cis*-IcPs (peak 4), however, remains unhydrolyzed even in part IIE.

Table 3: Specific Activities for the R_p and S_p Stereoisomers of DPPsI, Rate Constants, and the Stereoselectivity Ratio for WT and R69K

enzyme	specific activity for R_p (U/mg)	specific activity for S_p (U/mg)	k_{R_p} (μM^{-1} min^{-1})	k_{S_p} (μM^{-1} min^{-1})	selectivity k_{R_p}/k_{S_p}
WT	1100	0.014	13.5	8.5×10^{-5}	1.6×10^5
R69K	0.14	0.018	1.7×10^{-3}	1.1×10^{-4}	16

In the third experiment [Figure 5 (IIIA−D)], the R69K mutant (0.45 unit) was added to the same mixture of stereoisomers to see how the stereoselectivity of the mutant changed with respect to WT. Comparison between the results of the second and third experiments clearly indicates that, while the formation of peak 3 in the third experiment is slower than that in the second experiment, the formation of peak 4 is faster in the third experiment. These results clearly indicated a relaxation in the stereoselectivity for the R69K mutant.

The rates of conversion of the R_p isomer to the *trans*-IcPs product and the S_p isomer to *cis*-IcPs were then estimated from the ^{31}P NMR spectra shown in Figure 5 for both WT and R69K. The second-order rate constants for the R_p and S_p stereoisomers of WT and the R69K mutant were then calculated from these data and are summarized in Table 3. The data shown in Table 3 clearly indicate that the stereoselectivity, k_{R_p}/k_{S_p}, is relaxed by a factor of 10^4 in R69K. The mechanistic significance of this result is addressed in the Discussion.

DISCUSSION

Advantages of Continuous Assay Using DPsPI. We have developed a spectrophotometric assay using a phosphorothioate analogue as a substrate. Others (Hendrickson et al., 1992; Leigh et al., 1992; Shandishar et al., 1991a,b) have also used substrate analogues to develop continuous assays. These previously used analogues, hexadecylthiophosphoryl-1-*myo*-inositol (C_{16}S-PI) and *myo*-inositol 1-(4-nitrophenyl phosphate) (NPIP), have V_{max} values of 6.56 and 650 μmol min^{-1} mg^{-1}, respectively. NPIP is a water soluble analogue which does not form micelles and therefore does not present a water/lipid interface as the enzyme normally encounters. This is probably reflected in a high K_m for NPIP (5 mM). As such, NPIP is not a suitable analogue for detailed mechanistic studies, especially in comparing WT to mutants. C_{16}S-PI does have a hydrophobic moiety and thus a low K_m (0.011 mM), but the hydrophobic moiety is an alkyl chain rather than a diacylglycerol. DPsPI is the most similar to the structure of DPPI, with only a sulfur atom replacing an oxygen atom. It is thus far the best analogue used for a continuous assay for PI-PLC.

Our continuous assay is also validated by an almost 1:1 correspondence in activities between the specific activity assay and our continuous assay. For example, the D67A

mutant shows a 1.5-fold increase in activity as measured by the specific activity assay. The same mutant exhibits a 2-fold increase with respect to WT in the continuous assay. Likewise, the R69K mutant displays a 1300-fold decrease in activity in comparison to WT using the specific activity assay, while the continuous assay reveals a 1800-fold decrease for this mutant with respect to WT. Thus, we conclude that DPsPI is the best substrate analogue available for a continuous assay of PI-PLC activities. However, since DPsPI was used in the form of mixed micelles with DHPC, the V_{max} and K_m values should be considered apparent values.

Structural and Functional Roles of Asp-67. The activity of the D67A mutant toward PI (Table 1) is slightly higher than that of WT. The data regarding its conformational stability are somewhat difficult to interpret. The $\Delta G_d^{H_2O}$ value indicates that it is significantly less stable than WT (Table 2). However, the *m* value for D67A denaturation is significantly different than the *m* value of WT, and the $D_{1/2}$ Gdn-HCl concentrations for both WT and D67A are similar. This suggests that D67A is more susceptible to Gdn-HCl as a denaturant than WT but does not mean that its structure is significantly perturbed. The one-dimensional NMR data (data not shown) and the two-dimensional NMR experiments (data not shown) suggest that the global structure of D67A is similar to WT. From the crystal structure (Figure 2), Heinz et al. (1995) proposed that Asp-67 is involved in a hydrogen bond with Arg-69, possibly stabilizing the charge in the absence of substrate. Both Asp-67 and Arg-69 are highly conserved residues in the bacterial PI-PLC family (Daugherty & Low, 1993). While our results indicate that Arg-69 is critically important for catalysis as described in the next section, they suggest that Asp-67 does not play a significant role in the catalysis or the structural integrity of PI-PLC.

Structural and Functional Roles of Arg-69. The mutants of residue Arg-69 show little global conformational change when compared to WT. The mutation to alanine at this site exhibits the largest difference in the NOESY spectrum (data not shown) as compared to WT. The smaller number and lower intensity of NOE cross-peaks suggest that the R69A mutant's conformational mobility is increased with respect to that of WT. The global conformation should not have been perturbed since the overall pattern of detectable peaks resembles that of WT. This mutant also has slightly less conformational stability than WT as shown by its $\Delta G_d^{H_2O}$ value (Table 2). Both R69K and R69M have similar conformational stabilities with respect to WT as judged by their $\Delta G_d^{H_2O}$ values, and both mutants show virtually identical NOESY spectra (data not shown). The significantly decreased activities (10^3-10^4-fold) of the mutants at position 69 with respect to WT, and conserved global structures, indicate that Arg-69 is intimately involved in catalysis. The importance of the conservation of the positive charge is shown by the higher activity and structural integrity of the lysine mutant. The exact position of this positive charge is obviously important as indicated by the significantly lower activity of the lysine mutant compared to that of WT (Table 1). Heinz et al. (1995) proposed Arg-69 to be involved in the stabilization of the negative charge on the pentacoordinate phosphate group in the transition state. However, the crystal structure solved by Heinz et al. (1995) is a PI-PLC cocrystal with *myo*-inositol which lacks the phosphodiacylglycerol moiety. The experimental evidence on the interaction between Arg-69 and the phosphate group is provided by the stereochemical studies discussed in the following section.

Arginine-69 Interacts with the Phosphate Moiety of Phosphatidylinositol. It has been previously demonstrated (Bruzik et al., 1992) that PI-PLC lacks stereorecognition toward the 1,2-diacylglycerol moiety of phosphatidylinositol. It has been shown, however (Lin & Tsai, 1989; Lin et al., 1990), that PI-PLC is stereospecific toward the phosphate moiety of phosphatidylinositol and selectively utilizes the R_p isomer of DPPsI instead of the S_p isomer. Our previous work, however, did not quantitatively determine the degree of stereoselectivity. The data presented in Table 3 indicate that PI-PLC favors (R_p)-DPPsI over (S_p)-DPPsI by a factor of 1.6×10^5. To the best of our knowledge, this is the highest stereoselectivity toward R_p and S_p isomers of phosphorothioate analogues that have been quantitatively measured and reported. The result is particularly intriguing since the catalysis by *B. thuringiensis* PI-PLC does not involve a divalent metal ion. One would expect that the metal−phosphate interaction is a likely mechanism for the observed stereoselectivity.

As shown by our specific activity assay (Table 1), the activity of R69K toward DPPI decreases by 3 orders of magnitude relative to the activity of WT PI-PLC. The activity of R69K toward (R_p)-DPPsI decreases further (Table 3), by 4 orders of magnitude. On the other hand, the activity of R69K toward (S_p)-DPPsI is comparable to that of WT. Consequently, the stereoselectivity of R_p:S_p is relaxed by 4 orders of magnitude, from 1.6×10^5 for WT to 16 for R69K. Such a large change in the stereoselectivity toward DPPsI is strong evidence that the side chain of Arg-69 interacts directly with the phosphate moiety of phosphatidylinositol. Since the effect is mainly on the rate of catalysis, the interaction should occur at the transition state, which is likely to be a pentacovalent species.

In the case of adenylate kinase, we have also shown that stereoselectivity for the conversion of AMPS to (R_p)- or (S_p)-ADPαS can be manipulated by site-directed mutagensis (Jiang et al., 1991; Dahnke et al., 1991). The S_p:R_p ratio for WT is 95:5, which is completely reversed upon R44M mutation and enhanced to 99.5:0.5 upon R97A mutation. It should be noted that, in the case of adenylate kinase and AMPS, the choice the enzyme faces is between two diastereotopic oxygen atoms, while in PI-PLC and DPPsI, the choice is between two diastereomers. The degree of stereoselectivity and the degree of change upon mutation are both more dramatic for PI-PLC than adenylate kinase.

Conclusions. We have developed a new assay method using DPsPI/DHPC mixed micelles as substrate, which has allowed us to obtain quantitative kinetic data for WT PI-PLC and several mutants. The kinetic data, coupled with structural analyses by NMR and CD, allowed us to examine the structural and functional roles of both Asp-67 and Arg-69, which are located near the inositol binding site. The results indicate that Arg-69 is critically important for transition state stabilization. Stereochemical analysis using DPPsI analogues led us to further pinpoint that Arg-69 interacts directly with the phosphate moiety of the substrate. The degree of stereoselectivity toward the diastereomers of phosphorothioate analogues and the degree of change in the stereoselectivity upon R69K mutation are both among the highest observed for all enzymes.

NOTE ADDED IN PROOF

The synthesis of DPsPI, cited as "to be described elsewhere," has now been published (Mihai et al., 1997). In addition, the synthesis of the dimyristoyl analogue of DPsPI and its use for the kinetic assay of PI-PLC have also been published by others (Hendrickson et al., 1996).

ACKNOWLEDGMENT

We thank Xiaokui Mo for purifying some of the WT PI-PLC used in this study.

SUPPORTING INFORMATION AVAILABLE

Figure 1 showing the one-dimensional NMR spectra of WT and mutant enzymes, Figure 2 comparing the two-dimensional NOESY spectra of WT and mutant PI-PLCs, and Figure 3 depicting the $^{15}N-^{1}H$ HSQC spectrum of wild-type PI-PLC at 600 MHz (4 pages). Ordering information is given on any current masthead page.

REFERENCES

Bax, A., Ikura, M., Kay, L. E., Torchia, D. E., & Tschudin, R. (1990) *J. Magn. Reson. 86*, 304−318.

Berridge, M. J. (1987) *Annu. Rev. Biochem. 56*, 159−193.

Bodenhausen, G., & Ruben, D. J. (1980) *Chem. Phys. Lett. 69*, 185−189.

Bruzik, K. S., & Tsai, M.-D. (1994) *BioMed. Chem. Lett. 2*, 49−72.

Bruzik, K. S., Lin, G., & Tsai, M.-D. (1991) *ACS Symp. Ser. 463*, 172−185.

Bruzik, K. S., Morocho, A. M., Jhon, D.-Y., Rhee, S.-G., & Tsai, M.-D. (1992) *Biochemistry 31*, 5183−5193.

Cheng, H. F., Jiang, M. J., Chen, C. L., Liu, S. M., Wong, L. P., Lomasney, J. W., & King, K. (1995) *J. Biol. Chem. 270*, 5495−5505.

Dahnke, T., Jiang, R. T., & Tsai, M. D. (1991) *J. Am. Chem. Soc. 113*, 9388−9389.

Daugherty, S., & Low, M. G. (1993) *Infect. Immun. 61*, 5078−5089.

Dennis, E. A., Rhee, S. G., Billah, M. M., & Hannun, Y. A. (1991) *FASEB J. 5*, 2068−2077.

Drayer, A. L., & van Haastert, P. J. M. (1992) *J. Biol. Chem. 267*, 18387−18392.

Ellis, M. V., Sally, U., & Katan, M. (1995) *Biochem. J. 307*, 69−75.

Essen, L. O., Perisic, O., Cheung, R., Katan, M., & Wolliams, R. L. (1996) *Nature 380*, 595−602.

Greenfield, N., & Fasman, G. D. (1969) *Biochemistry 8*, 4108−4120.

Griffith, O. H., Volwerk, J. J., & Kuppe, A. (1991) *Methods Enzymol. 197*, 493−502.

Heinz, D. W., Ryan, M., Bullock, T. L., & Griffith, O. H. (1995) *EMBO J. 14*, 3855−3863.

Hendrickson, E. K., Johnson, L. J., & Hendrickson, H. S. (1991) *BioMed. Chem. Lett. 1*, 615−618.

Hendrickson, H. S., Hendrickson, E. K., Johnson, L. J., Khan, T. H., & Chial, H. J. (1992) *Biochemistry 31*, 12169−12172.

Hendrickson, H. S., Banovetz, C., Kirsch, M. J., & Hendrickson, E. K. (1996) *Chem. Phys. Lipids 84*, 87−92.

Ikezawa, H. (1991) *Cell Biol. Int. Rep. 15*, 115−1131.

Iwasaki, Y., Niwa, S., Nakano, H., Nagasawa, T., & Yamane, T. (1994) *Biochim. Biophys. Acta 1214*, 221−228.

Jhon, D.-Y., Lee, H.-H., Park, D., Lee, C.-W., Lee, K.-H., Yoo, O. K., & Rhee, S. G. (1993) *J. Biol. Chem. 268*, 6654−6661.

Jiang, R. T., Dahnke, T., & Tsai, M.-D. (1991) *J. Am. Chem. Soc. 113*, 5485−5486.

Kessi, J., Poirée, J.-C., Wehrli, E., Bachofen, R., Semenza, G., & Hauser, H. (1994) *Biochemistry 33*, 10825−10836.

Koke, J. A., Yang, M., Henner, D. J., Volwerk, J. J., & Griffith, O. H. (1991) *Protein Expression Purif. 2*, 51−58.

Kuppe, A., Evans, L. M., McMillen, D. A., & Griffith, O. H. (1989) *J. Bacteriol. 171*, 6077−6083.

Lee, C.-W., Park, D. J., Lee, K.-H., Kim, C. G., & Rhee, S. G. (1993) *J. Biol. Chem. 268*, 21318−21327.

Lee, S. B., & Rhee, S. G. (1995) *Curr. Opin. Cell Biol. 7*, 183−189.

Leigh, A. J., Volwerk, J. J., Griffith, O. H., & Keana, J. F. W. (1992) *Biochemistry 31*, 8978−8983.

Lin, G., & Tsai, M. D. (1989) *J. Am. Chem. Soc. 111*, 3099−3101.

Lin, G., Bennet, F., & Tsai, M. D. (1990) *Biochemistry 29*, 2747−2757.

Low, M. G. (1990) in *Molecular and Cell Biology of Membrane Proteins: Glycolipid Anchors of Cell Surface Proteins* (Turner, A. J., Ed.) pp 35−54, Ellis Horwood, New York.

Mihai, C., Mataka, J., Riddle, S., Tsai, M.-D., & Bruzik, K. S. (1997) *Bioorg. Med. Lett. 7*, 1235−1238.

Pace, C. N., Shirley, B. A., & Thomson, J. A. (1989) in *Protein Structure, a Practical Approach* (Creighton, T. E., Ed.) pp 311−330, IRL Press at Oxford University Press, Oxford, England.

Piotto, M., Saudek, V., & Sklenar, V. (1992) *J. Biomol. NMR 2*, 661−666.

Rana, R. S., & Hokin, L. E. (1990) *Phys. Rev. 70*, 115−164.

Rhee, S. G., & Choi, K. D. (1992) *J. Biol. Chem. 267*, 12393−12396.

Rhee, S. G., Suh, P. G., Ryu, S. H., & Lee, S. Y. (1989) *Science 244*, 546−550.

Richards, F. M., & Wyckoff, H. W. (1970) Bovine pancreatic ribonuclease, in *The Enzymes* (Boyer, P. D., Ed.) pp 647−806, Academic Press, New York.

Ross, T., & Majerus, P. W. (1986) *J. Biol. Chem. 261*, 11119−11123.

Sambrook, J., Fritsch, E. F., & Maniatis, T. (1989) *Molecular Cloning, A Laboratory Manual*, 2nd ed., Cold Spring Harbor Laboratory Press, Plainview, NY.

Shandishar, M. S., Volwerk, J. J., Griffith, O. H., & Keana, J. F. W. (1991a) *Chem. Phys. Lipids 60*, 101−110.

Shandishar, M. S., Volwerk, J. J., Keana, J. F. W., & Griffith, O. H. (1991b) *Anal. Biochem. 198*, 10−14.

Sklenar, V., Piotto, M., Leppik, K., & Saudek, V. (1993) *J. Magn. Reson. 102*, 241−245.

Steiger, S., & Brodbeck, U. (1991) *Biochimie 73*, 1179−1186.

Volwerk, J. J., Wetherwax, P. B., Evans, L. M., Kuppe, A., & Griffith, O. H. (1989) *J. Cell. Biochem. 39*, 315−325.

Volwerk, J. J., Shandishar, M. S., Kuppe, A., & Griffith, O. H. (1990) *Biochemistry 29*, 8056−8062.

Volwerk, J. J., Filthuth, E., Griffith, O. H., & Jain, M. K. (1994) *Biochemistry 33*, 3364−3474.

Yu, L., & Dennis, E. A. (1991) *Methods Enzymol. 197*, 65−75.

BI962866G